3 Structural Biology Research Center

3-1 Introduction

The Structural Biology Research Group was formed in May 2000. The aims of the research group are user support in synchrotron-radiation X-ray crystallography of macromolecules, the development of highly advanced techniques, and in-house research in structural biology. The group has grown steadily during the last six years, with the number of members increasing from four (one Professor and three Research Associates) to about thirty (Figure 1). The core staff members of the group are currently the group leader Professor Soichi Wakatsuki, Associate Professor Ryuichi Kato, two Associate Lecturers (Noriyuki Igarashi and Masahiko Hiraki), and three Research Associates (Naohiro Matsugaki, Masato Kawasaki and Yusuke Yamada). The structural biology building had been previously enlarged from 429 m^2 to 643 m^2 in area, and was re-extended to about 850 m^2 in FY2006 to accommodate the increasing number of group members. While about half of the members are engaged in beamline operation/development and the remaining half in biological research, the synergy between these two activities is a unique aspect of this group. Along with the recent change of the status of KEK from a governmental institute to an agency in April 2004, the Structural Biology Research Group became the Structural Biology Research Center in May 2003. So far four graduate students have successfully obtained a Ph.D. based on their studies in the Structural Biology Research Center. Two graduate students at the Graduate University for Advanced Studies (SOKENDAI) are currently carrying out their own research relevant to the group's research fields under the guidance of the group staff.

During FY2001-FY2003, a "Special Coordination Funds for Promoting Science and Technology" award from MEXT (the Ministry of Education, Culture, Sports, Science and Technology) supported the activities of our group together with other universities (Hokkaido Univ., The Univ. of Tokyo, Kyoto Univ., and Osaka Univ.) and the research institute of NHK (Japanese National Broadcasting Corporation). We built and commissioned a new high-throughput beamline, BL-5A, developed an assortment of technologies for the automated handling of protein crystals, constructed a prototype of a next-generation two-dimensional X-ray HARP (high-gain avalanche rushing amorphous photoconductor) detector, and developed software to facilitate rapid and accurate structure determination. We also made improvements to the experimental environment associated with the beamlines and sample-preparation laboratories using the same research fund. Subsequently, a five-year national project "Protein 3000" was started by MEXT in FY2002. This project consists of two programs; a "Comprehensive Program" carried out by RIKEN and "Individual Analysis Programs" carried out by eight consortia of universities and institutes including the Structural Biology Research Center. In addition, in FY2004 a new research and development program "Development of Systems and Technology for Advanced Measurement and Analysis" was launched by JST (Japan Science and Technology Agency). We proposed a project to develop a next-generation detector coupled with a micro-focus beamline. This project was selected and commenced in the same year for an initial 3 years. In this project, we have developed a new beamline, BL-17A, optimized for data collection from small crystals, and an advanced prototype of an X-ray HARP detector in collaboration with NHK Engineering Service (NHK-ES) and associated companies.

Figure 1
The members of Structural Biology Research Center pictured at the entrance to the Structural Biology Building.

3-2 Protein 3000 Project — Individual Analysis Programs —

FY2006 was the last year of the five-year Protein 3000 Project. The Structural Biology Research Center serves as one of the eight consortia of the national project, pursuing structural and functional analyses in the field of post-translational modification and transport. Our consortium consists of eleven universities and four research institutes (Table 1).

Cell signaling and intracellular trafficking are the means by which eukaryotic cells deliver cargo proteins to various organelles, cell membranes, and extracellular destinations (Fig. 2). During the trafficking process, more than half of the eukaryotic proteins undergo post-translational processing and modification such as glycosylation. Accurate distribution and modification of the proteins are crucial for a range of cellular functions and activities. A more profound understanding of the biological and biomedical function of transport and modifica-

Functional Analyses	Intracellular trafficking	Akihiko Nakano (RIKEN, Univ. of Tokyo) Kazuhisa Nakayama (Kyoto Univ. Pharmaceutical) Hiroshi Ohno (RIKEN Laboratory of Epithelial Immunobiology), Hiroaki Kato (Kyoto Univ. Pharmaceutical) Masayuki Murata (Univ. of Tokyo, Arts and Sciences) Syuya Fukai (Tokyo Inst. of Technology) Soichi Wakatsuki (KEK-PF)
	Post-translational modification	Shogo Oka (Kyoto Univ. Pharmaceutical) Naoyuki Taniguchi (Osaka Univ. Medicine) Yoshifumi Jigami (AIST) Koichi Kato (Nagoya City Univ. Pharmaceutical) Sumihiro Hase (Osaka Univ. Science) Soichi Wakatsuki (KEK-PF) Tamao Endo (Tokyo Metropolitan Institute of Gerontology) Kenji Yamamoto (Kyoto Univ. Graduate School of Biostudies) Akira Kurosaka (Kyoto Sangyo Univ. Faculty of Engineering)
	Medical applications	Tatsuo Shioda (Osaka Univ. Institute for Microbial Diseases) Hirohito Tsubouchi (Kagoshima Univ. Medical and Dental Sciences) Akio Ido (Kyoto Univ. Hospital. Translational Research Center)
Structural Biology	X-ray crystallography	Takamasa Nonaka (Nagaoka Univ. of Technology) Nobutada Tanaka (Showa Univ. Pharmaceutical) Hiroaki Kato (Kyoto Univ. Pharmaceutical) Shuya Fukai (Tokyo Inst. of Technology) Soichi Wakatsuki (KEK-PF)
	NMR, Small angle X-ray scattering, Bioinformatics	Koichi Kato (Nagoya City Univ. Pharmaceutical) Mikio Kataoka (Nara Inst. of Science and Technology) Kei Yura (JAERI CCSE)

Table 1 Members of the "Post-Translational Modification and Transport" network in Protein 3000 Project.

tion proteins is indispensable for making progress in the medical treatment of human diseases.

To facilitate the current research program, the Structural Biology Research Center has taken the lead by coordinating the research network. As part of the project, we have sought to maximize the efficiency of the large-scale expression, purification, and crystallization of proteins by trying to eliminate the bottlenecks in each process. Crystallographic studies using synchrotron X-ray radiation are conducted at KEK-PF, NMR experiments at Nagoya City University and small-angle X-ray scattering experiments at Nara Institute of Science and Technology (Table 1). Each structural analysis project maintains close contact with the groups responsible for functional analyses. Our initial research plan was to accomplish the structural and functional analyses of over 70 proteins in five years. At the end of the project, the number of structures determined has reached over 250, with a total of 296 published papers (Table 2). Thirteen domestic and two international patent applications have been submitted based on our R&D and structural and functional studies of the target proteins. Since the total number of structures determined as part of the Protein 3000 Project has exceeded 3,000, the project has finished with success, with our consortium making a significant contribution to the results.

KEK-PF is one of the two synchrotron-radiation facilities with high-throughput protein crystallography beamlines in Japan. To promote the Protein 3000 Project, the Structural Biology Research Center has established an operation scheme to reserve about 30% of the beam time at our beamlines for users of the eight university consortia under an S2 proposal (see page 123). As summarized in Table 3, a total of 327 days of beam time has been allocated to users since the beginning of the project. A web-based beam time reservation system has also been developed for efficient beam-time allocation.

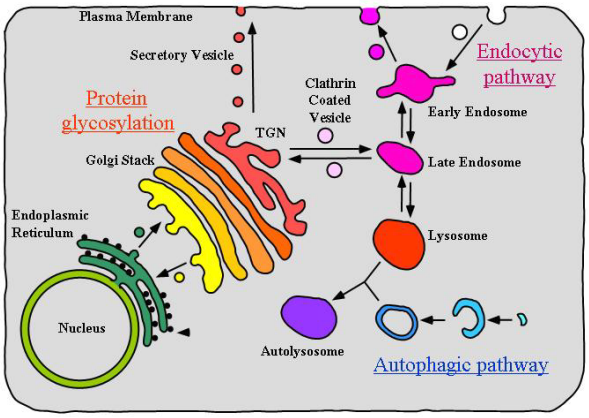

Figure 2
Schematic drawing of protein glycosylation and transport in cells.

Table 2 Result of the "Posttranslational Modification and Transport" network in Protein 3000 Project.

	Number
Number of structures solved	254
Number of PDB* deposited	171
The others	83
Number of publised papers	296
Number of submitted patent (international)	15 (2)

*PDB, international structural database for bio-macromolecule

Table 3 Beam time used at KEK-PF in Protein 3000 Project.

Network Committee	FY 2003	FY 2004	FY 2005	FY2006	Total
Metabolism	12	25	15.5	23.5	76
Development and Cell differentiation	3	8.5	10.5	12.5	34.5
Transcription and Translation (Hokkaido University)	1	7.5	11.5	15.5	35.5
Transcription and Translation (Yokohama City University)	8	14	8.75	9	39.75
Higher Order Biological Functions (Kyoto Univ.)	0	1	7.5	10.5	195
Signal Transduction (Hokkaido Univ.)	1	3.5	5.5	11	21
Brain and Neurology (Osaka Univ.)	3	8	11	15.5	37.5
Protein Transport and Modification (KEK-PF)	13	18	16.5	16.5	64
Total (days)	41	85.5	86.75	114	327.25

3-3 Highlights on In-House Structural Biology Research

Mammalian Eap45 GLUE domain directly interacts with ubiquitin

The down-regulation of membrane proteins is triggered by their mono-ubiquitination, whereas that of soluble proteins is triggered by the K48-linked ubiquitin (Ub) chain. Hrs/STAM/Eps15, ESCRT-I, and ESCRT-II are known to interact with Ub, and their Ub-interaction ability is essential for mono-Ub mediated down-regulation. The Ub-interaction mechanism has been revealed by structural studies, however, that of mammalian ESCRT-II remained unclear because it does not have a domain which corresponds to the Ub-binding domain (NZF domain) of yeast ESCRT-II. In our previous work, we revealed that a GLUE domain of subunit Eap45 in ESCRT-II is the Ub-binding domain of mammalian ESCRT-II. We also demonstrated that the Eap45-GLUE interacts with a lipid, phosphatidyl inositol (PI), for localization of ESCRT-II on endosomal membranes [1].

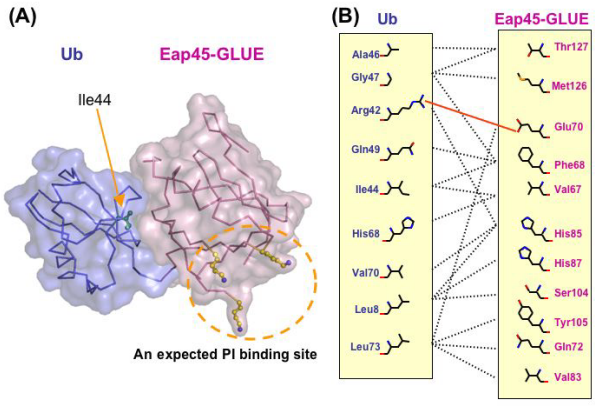

Figure 3
(A) Overall structure of the complex between mouse Eap45 GLUE (magenta) and Ub (slate). The Ile44 of Ub is shown as a green ball-and-stick model. The residues which are expected to be involved in phosphoinositide (PI) binding are shown as ball-and-stick models, with yellow representing carbon atoms, and blue representing nitrogen atoms. (B) Schematic diagram of the GLUE-Ub interaction. The broken black lines indicate contacts between the Eap45-GLUE and Ub molecules, and the solid red line indicates a salt bridge.

In order to reveal the Ub-interaction mechanism of Eap45-GLUE, we solved the crystal structure of a mouse Eap45-GLUE/Ub complex [2]. The structure is a PH domain fold, similar to that of the yeast Vps36-GLUE domain (Fig. 3A). The interaction surface of the Ub molecule consists of Leu8, Arg42, Ile44, Ala46, Gly47, Gln49, His68, Val70 and Leu73, involving the common interaction surface of Ub termed the "Ile44 surface". The Ub interacts with Val67, Phe68, Glu70, Val83, Gln72, Met126, His85, His87, Ser104, Tyr105 and Thr127 of Eap45-GLUE, burying 1000 Å^2 of their accessible surface area (Fig. 3B). In addition to the hydrophobic interactions, GLUE Glu70 is involved in electrostatic interactions with Ub Arg42. Importantly, the revealed Ub-binding site of Eap45-GLUE is a completely different position from the expected PI-binding site (Fig. 3A), suggesting that Eap45-GLUE binds to Ub and PI-simultaneously. As the yeast Vps36 has also been shown to bind Ub and IP independently, the simultaneous-binding ability of Eap45-GLUE to both Ub and the endosomal membrane might be essential for the down-regulation of membrane proteins. For more details see the highlight report of this issue on page 39.

Recognition mechanism of small GTPase Rab11 by FIP3

Small GTPases belonging to the Ras-like superfamily regulate endocytotic membrane trafficking, and ARF and Rab proteins participate in multiple stages of trafficking along the exocytic and endocytic pathways. ARFs initiate the budding of coated carrier vesicles by recruiting coat protein complexes onto donor membranes, whereas Rabs regulate the targeting and docking/fusion of vesicles with acceptor membranes. Rab11, which is one of the Rab proteins, regulates the recycling of endosomes

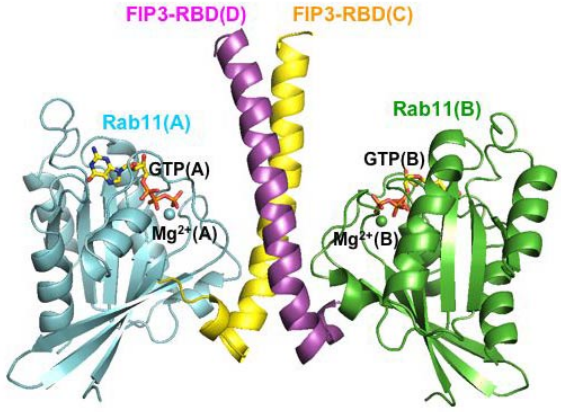

Figure 4
(A) Crystal structure of the Rab11-FIP3-RBD complex. The asymmetric unit contains two Rab11 (molecules A; cyan and B; green) and two FIP3-RBD (molecules C; yellow and D; purple) molecules. GTP and Mg^{2+} ions are shown as ball-and-stick models.

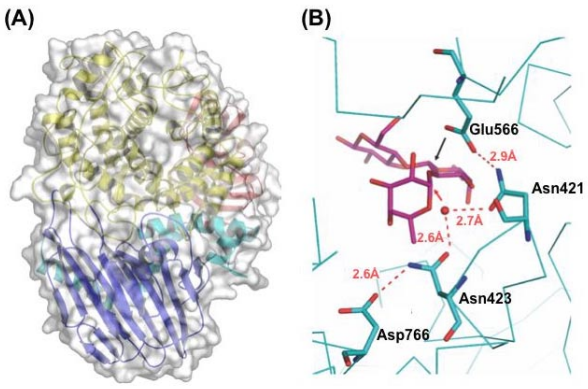

Figure 5
(A) Overall structure of the catalytic (Fuc) domain of AfcA fucosidase. (B) Proposed catalytic reaction mechanism. The substrate 2'-fucosyllactose and the amino acid residues which are involved in the proton transfer are shown as rod models. The direction of the nucleophilic attack by the activated water molecule is shown as a red arrow, and the direction of the proton transfer by Glu566 is shown as a black arrow.

to the plasma membrane via interactions with the Rab11 family of interacting proteins (FIPs). FIPs contain a highly conserved Rab binding domain (RBD) at their C termini.

To understand the recognition mechanisms of Rab11 by FIPs, we determined the crystal structure of Rab11 in complex with the RBD of FIP3 at 1.75Å resolution [3]. The long amphiphilic alpha-helix of FIP3-RBD forms a parallel coiled-coil homodimer, with two symmetric interfaces with two Rab11 molecules (Fig. 4). The hydrophobic side of the FIP3-RBD helix is involved in homodimerization and mediates the interaction with the Rab11 switch 1 region. The hydrophilic side of the amphiphilic helix of FIP3-RBD interacts with the switch 2 region of the Rab11 molecule. The side chains of Arg74 and Arg82 in switch 2 form salt bridges with Asp739 and Glu747, respectively. Interestingly, the side chain of Tyr80 points inward, thereby forming an intramolecular hydrogen bond with the main chain carbonyl of Leu16. As a result, Rab11 forms a characteristic large hydrophobic pocket surrounded by Ile76, Ala79, Tyr80 of switch 2, and Trp65 of the interswitch region, which accommodates the large side chain of FIP3-RBD Met746. In summary, the bivalent interaction of FIP3 with Rab11 at the C terminus allows FIP3 to coordinately function with other binding partners, including ARFs. For more details see the highlight report of this issue on page 41.

Structural basis of the catalytic reaction mechanism of novel 1,2-α-L-Fucosidase (AfcA) from a lactic acid bacterium

1,2-α-L-Fucosidase (AfcA), which hydrolyzes the glycosidic linkage of Fucα1-2Gal was recently isolated from a lactic acid bacterium, Bifidobacterium bifidum. It was classified as the first member of the novel glycoside hydrolase family 95 (GH95) using the CAZY server (see http://www.cazy.org/CAZY/). AfcA has 1,959 amino acids and consists of three domains: an N-terminal domain with unknown function, a catalytic domain (Fuc-domain), and a C-terminal bacterial Ig-like domain. The recombinant Fuc-domain which has 896 amino acids showed 1,2-α-L-fucosidase (EC 3.2.1.63) activity. To understand the molecular reaction mechanism of this enzyme, we determined the X-ray crystal structures of the Fuc-domain in unliganded and complexed forms with deoxyfuconojirimycin (inhibitor), 2'-fucosyllactose (substrate), and L-fucose and lactose (products) at 1.12-2.10 Å resolution [4].

The AfcA Fuc domain is composed of four regions, an N-terminal β region, a helical linker, an $(\alpha/\alpha)_6$ helical barrel domain, and a C-terminal β region (Fig. 5A), an arrangement similar to bacterial phosphorylases. In the complex structures, the ligands were buried in the central cavity of the helical barrel domain. Structural analyses in combination with mutational experiments revealed that the highly conserved Glu566 likely acts as a general acid catalyst. However, no carboxylic acid residue is found at the appropriate position for a general base catalyst. Instead, a water molecule stabilized by Asn423 in the substrate-bound complex is suitably located to perform a nucleophilic attack on the C1 atom of L-fucose moiety in 2'-fucosyllactose, and its location is nearly identical to the O1 atom of beta-L-fucose in the products-bound complex. Based on these data, we proposed a novel catalytic reaction mechanism of AfcA (Fig. 5B).

References

[1] T. Slagsvold, R. Aasland, S. Hirano, K.G. Bache, C. Raiborg, D. Trambaiolo, S. Wakatsuki and H. Stenmark, *J. Biol. Chem.*, **280** (2005) 19600.
[2] S. Hirano, N. Suzuki, T. Slagsvold, M. Kawasaki, D. Trambaiolo, R. Kato, H. Stenmark and S. Wakatsuki, *Nature Struct. Mol. Biol.*, **13** (2006) 1031.
[3] T. Shiba, H. Koga, H.-W. Shin, M. Kawasaki, R. Kato, K. Nakayama and S. Wakatsuki, *Proc. Natl. Acad. Sci.*, **103** (2006) 15416.
[4] M. Nagae, A. Tsuchiya, T. Katayama, K. Yamamoto, S. Wakatsuki and R. Kato, *J. Biol. Chem.*, **282** (2007) 18497.

3-4 Beamline and Robotics

Beamline BL-17A was newly constructed and opened for general users in FY2006 (Fig. 6), supported by the "Development of Systems and Technology for Advanced Measurement and Analysis" program (FY2004-2007) of JST. The new beamline was designed for micro-crystal structure analysis. In addition, an intense lower energy beam at around 6 keV is used for structure determination by Single wave length Anomalous Dispersion (SAD) phasing with light atoms. The source of the beamline is a newly developed short-gap undulator installed in one of the four short straight sections of the PF 2.5-GeV ring. The measured focused beam size (FWHM) using the K-B mirror system is about 0.03 mm (V) × 0.23 mm (H). The photon flux at 12 keV with the collimation slit set to widths of 100 μm^2 and 20 μm^2 were 8×10^{10} and 7×10^9 photons/sec respectively. This performance is high enough for micro-crystal structure analysis [1]. However, we observed instabilities of about 10% in the beam intensity, which could be classified into 5 different forms: (1) a spike-like intensity change every few minutes, (2) a high frequency fluctuation, (3) an irregular step-like intensity change, (4) intensity change depending on the movement of heavy materials around the optics, and (5) a long term beam drift. The following solutions were considered; (1) He purge operation of the monochromator liquid nitrogen flow, (2) reduction of vibration around the optics, (3) improvement of the ring operation, (4) translocation of the mirror optics on the stable floor frame, and (5) introduction of an X-ray beam feedback system. So far, the major parts of these solutions have been implemented, and the instabilities have successfully been reduced to within 2%. Further optimization and stabilization are under way on the ring operation and the beamline optics.

A newly fabricated micro-channel Si crystal (Fig. 7A) was installed in the monochromator of BL-5A. The beam intensity at the sample position was increased by a factor of 1.5 due to better performance in reducing the heat load on the surface of the crystal. At AR-NW12A, the X-ray CCD detector (ADSC Quantum 210) was upgraded to a Quantum 210r during the summer shutdown (Fig. 7B). The improved electronics reduce the readout noise, allowing weaker diffractions to be measured. In addition, the readout time has become shorter. Motorized cryo-stream nozzles and pneumatic annealing screens have been installed into all the protein crystallography beamlines (Fig. 7C). The position of the cryo-nozzle is optimized automatically for both data collection and sample exchange.

We have decided to construct a new beamline in a partnership with Astellas Pharma Inc., Japan in the PF-AR NE3 section, which will be dedicated to drug design. The new beamline is expected to perform better than the existing high-throughput beamlines BL-5A/AR-NW12A. Construction of the beamline will be completed in March 2009, and general use will commence in April 2009. Part of the beamtime will be available for academic users. The details of the beamline AR-NE3 are given on page 66.

For high-throughput operation of the beamlines, we have developed sample exchange robots based on the SAM system (Stanford synchrotron radiation laboratory automated mounting system), and installed them at BL-5A and AR-NW12A. These two robots have been open to users since October 2006. The use of a 3rd robot for R&D started in April 2006, and a 4th robot was installed at BL-17A in February 2007 (Fig. 6). The three robots installed at the beamlines were used by 11.0% of users. A double-tongs system that can hold two samples simultaneously was implemented on the BL-5A robot. A result of preliminary experiments showed that the time required for sample exchange was reduced to 10 sec from 70 sec.

Figure 6
Inside view of the experimental hutch of BL-17A. The sample exchange robot (SAM system) is located beside the diffractometor.

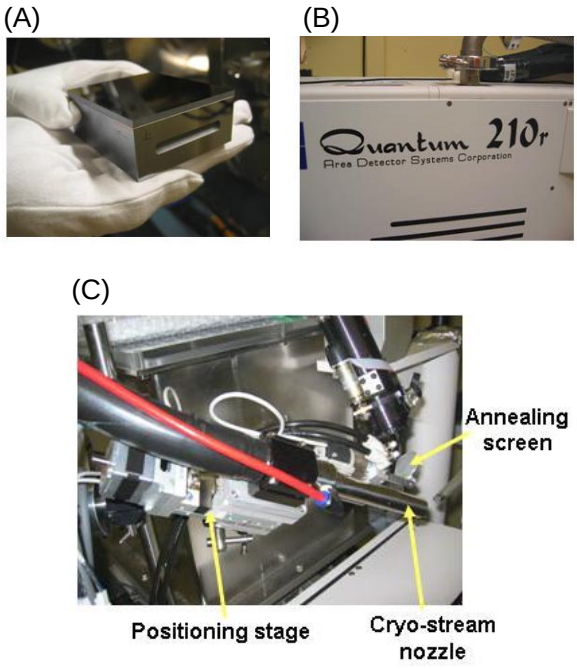

Figure 7
(A) The newly fabricated micro-channel Si crystal installed in BL-5A. (B) The upgraded ADSC Quantum 210r X-ray CCD detector at the AR-NW12A beamline. (C) The motorized cryo-stream nozzle and pneumatic annealing screen installed at BL-5A.

References

[1] N. Igarashi, N. Matsugaki, Y. Yamada, M. Hiraki, A. Koyama, K. Hirano, T. Miyoshi and S. Wakatsuki., *AIP Conf. Proc.*, **879** (2007) 812.

3-5 A New Measurement System for Protein Crystallography Combined with the Development of a Next-Generation X-Ray Area Detector

We are now developing a new measurement system for protein crystallography, based on an X-ray HARP - FEA (field emitter array) detector, a micro-focus beamline and a high-speed sample exchange robot. The system is optimized for micron-size protein crystals and for high-throughput data collection. This development project has been performed in collaboration with NHK-ES, and funded by JST under the "Development of Systems and Technology for Advanced Measurement and Analysis" program (FY2004-2007). A key of the project, the development of a high-gain, high-speed area detector based on HARP-FEA technology is described here. The developments of a micro-focus beamline and a high-speed sample exchange robot is described in the previous section (Fig. 6).

The main parts of the HARP-FEA detector are an amorphous selenium membrane and an FEA. The characteristics of the avalanche effect in the membrance and the single driven FEA show the following advantages over the currently available area detectors: (1) higher sensitivity, (2) higher spatial resolution, (3) a higher framing rate, and (4) lower noise and radiation hardness. In FY2006, we completed the development of two kinds of prototype: a Spindt-type and a HEED-type FEA detector (Fig. 8A). Fundamental evaluation of the detectors was performed at beamlines BL-14B, 14C, 17A, and AR-NE5A of the Photon Factory. The spatial resolution reached below 20 μm, with a dynamic range of over 9 bits at 30 Hz readout. The detectors showed sensitivities 10 times better than a fiber-optic coupled CCD detector at 14 keV, and 100 times better than a CsI-coupled CCD detector at 30 keV.

The prototype X-ray HARP-FEA detectors have been tested in diffraction experiments at the protein crystallography beamline BL-17A. A series of diffraction images with continuous rotation of the sample was recorded. The images were compared with those recorded using the existing fiber optics coupled CCD detector, and showed better spot separation. In addition the speed of data collection was remarkably higher. We are currently developing a synchronization interface between the HARP-FEA detector and the beamline control system.

The HARP detectors have also been tested for low-dose medical imaging and real-time phase-contrast imaging methods. One example is an X-ray phase-map measurement using a triple Laue-case (LLL) X-ray interferometer [1]. Although the application was performed with a HARP tube camera, the phase map of a rat liver was successfully obtained using the fringe scanning and phase unwrapping methods (Fig. 8B). This result demonstrates that the direct-sensing X-ray HARP cameras are useful for acquiring X-ray phase maps. Details are given in the highlight report on page 51 of this issue.

References

[1] K. Hirano, T. Miyoshi, N. Igarashi, T. Takeda, J .Wu, T. -T. Lwin, M. Kubota, N. Egami, K. Tanioka, T. Kawai and S. Wakatsuki, *Phys. Med. Biol.*, **52** (2007) 2545.

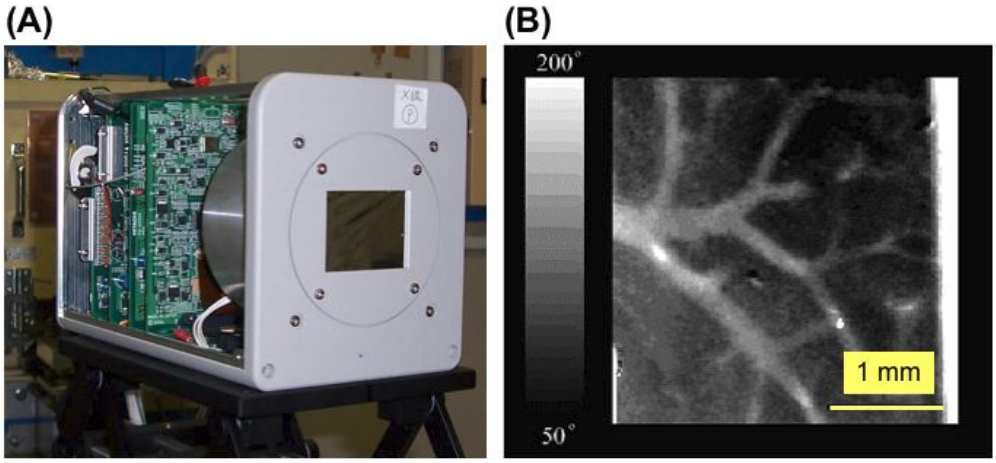

Figure 8
(A) View of the prototype X-ray HARP-FEA camera. (B) Phase-map image after background subtraction of a rat liver visualized using the X-ray HARP detector. The field of view is about 3 mm (H) × 3 mm (V). Trees of blood vessels are clearly visible. The minimum size of the blood vessels is estimated to be about 35 μm.